Article:

Jeebodh, A., Davison, B. orcid.org/0000-0002-6191-7301, McLaggan, M.S. orcid.org/0000-0002-4173-5615 et al. (3 more authors) (2024) Influence of continuous elastic lateral restraints on beams and beam-columns of steel-timber hybrid structures in fire. Fire Safety Journal, 146. 104172. ISSN 0379-7112

https://doi.org/10.1016/j.firesaf.2024.104172

Fire Safety Journal 146 (2024) 104172

Contents lists available at ScienceDirect

Fire Safety Journal

journal homepage: www.elsevier.com/locate/firesaf

Influence of continuous elastic lateral restraints on beams and beam-columns of steel-timber hybrid structures in fire

Aatish Jeebodh [a,*], Buick Davison [a], Martyn S. McLaggan [a], Ian Burgess [a], Danny Hopkin [b], Shan-Shan Huang [a]

[a] University of Sheffield, Sheffield, S1 3JD, UK
[b] OFR Consultants, The Manse, 44 South Bar, Banbury, Oxford, OX16 9AB, UK

ARTICLE INFO

Keywords:
Steel-timber hybrid structures
Lateral-torsional buckling
Continuous elastic restraints
Parametric study
Fire

ABSTRACT

With the climate crisis and pursuit of efforts to reduce embodied carbon impacts in the built environment, steel-timber hybrid structures have emerged as a sustainable form of framed construction which offer numerous benefits over the widely used and well-established steel-concrete hybrid structures. However, there are major concerns about the structural fire performance of such systems among various stakeholders in the construction industry, particularly for the design implications in terms of the lateral-torsional buckling behaviour and the degree of lateral restraint mobilised in the steel-to-timber connections. The screws that connect cross-laminated timber slabs to steel beams may provide a certain degree of restraining action in fire. However, further investigations are required to quantify the slip characteristics of such connections. In this study, it was found from existing literature that at the fire limit state, the continuous elastic lateral stiffness available to restrain the beam varies between approximately 500 kN/m/m and 2000 kN/m/m. Relying entirely on the screws and using this practical range of stiffness, a parametric study using Eurocode 3 design buckling resistance equations on 9 m simply supported span steel beams and beam-columns with span-to-depth ratios of about 10, 15, 20 and 25 was performed. The results indicate that designing such members as fully restrained in fire conditions may lead to unrealistic assumptions and unsafe structures.

1. Introduction

Steel-timber hybrid structures are innovative structural solutions that are being adopted for commercial office and mixed-use developments. This type of construction consisting of mass-timber cross-laminated timber (CLT) panels with non-combustible steel frames offer benefits such as sustainability with low embodied carbon impacts, dry construction, off-site fabrication, lightness, biophilic design, and long beam spans. However, the fire performance of such systems is a concern and there is uncertainty among industry practitioners regarding the susceptibility of the steel beams to lateral-torsional buckling instability in fire conditions [1,2], which is further exacerbated by the development of axial compression due to restrained thermal expansion [3].

In this type of structural system, the CLT panels are connected to steel beams using closely spaced self-tapping screws and from a structural perspective, these beams can be assumed to be supported laterally by a linear elastic foundation with uniform continuous stiffness k located at a distance a from the centroid of the section, as shown in Fig. 1. Researchers such as Flint [4], McCann et al. [5], and Belaid et al. [6] have shown improvement of the lateral-torsional buckling behaviour of steel beams with different types of restraints but studies with continuous elastic restraints in fire are lacking. This is because in conventional steel-concrete composite construction, the steel beams are normally assumed to be fully restrained by the concrete slab and restraints in other types of steel construction are generally discrete and at large spacings. Compared to unrestrained beams, which fail at moments close to the critical elastic moment, beams with continuous or closely spaced restraints and sufficient lateral stiffness capacity can achieve full plastic moment resistance [7]. Hence, the aim of this study is to investigate the influence of uniform continuous elastic restraints on steel beams and beam-columns in steel-timber hybrid structures at elevated temperatures. The objectives are: (i) to review the current lateral-torsional buckling resistance equations for partially restrained members, (ii) to assess the level of lateral stiffness mobilised by self-tapping screws based

* Corresponding author.
E-mail address: ajeebodh1@sheffield.ac.uk (A. Jeebodh).

https://doi.org/10.1016/j.firesaf.2024.104172
Received 27 November 2023; Received in revised form 23 February 2024; Accepted 2 May 2024
Available online 3 May 2024

on existing literature, and (iii) to perform a parametric study to determine the influence of continuous restraints on heated beams and beam-columns.

2. Theoretical background

This section provides an overview of the theoretical framework for the verification of lateral-torsional buckling of steel beams and beam-columns with uniform continuous elastic restraints at high temperature using current design equations in BS EN 1993-1-2 [8]. Existing analytical methods to determine the critical elastic moment and critical elastic load for both cases are also presented. A background knowledge of steel section classification with respect to slenderness, local buckling and plastic/elastic capacity is required to understand this section and a detailed explanation can be found in Ref. [9].

2.1. Lateral torsional buckling resistance of beams in fire

The design lateral torsional buckling resistance moment $M_{b,fi,t,Rd}$ at time t of a laterally unrestrained steel beam at elevated temperatures with a Class 1 or 2 cross-section can be determined from:

$$M_{b,fi,t,Rd} = \frac{\chi_{LT,fi} W_{pl,y} k_{y,\theta,com} f_y}{\gamma_{M,fi}} \tag{1}$$

where $\chi_{LT,fi}$ is the reduction factor for lateral torsional buckling in fire, $W_{pl,y}$ is the plastic modulus of the section, $k_{y,\theta,com}$ is the reduction factor for the yield strength at the maximum steel temperature in the compression flange, f_y is the yield strength of the steel section, and $\gamma_{M,fi}$ is the partial safety factor for material properties in fire, which is usually taken as 1.0.

The value of $\chi_{LT,fi}$ is determined using the following equation:

$$\chi_{LT,fi} = \frac{1}{\varphi_{LT,\theta,com} + \sqrt{\left(\varphi_{LT,\theta,com}\right)^2 - \left(\bar{\lambda}_{LT,\theta,com}\right)^2}} \tag{2}$$

with

$$\varphi_{\mathrm{LT},\theta,\mathrm{com}} = 0.5\left[1 + \alpha\bar{\lambda}_{LT,\theta,com} + \left(\bar{\lambda}_{LT,\theta,com}\right)^2\right] \tag{3}$$

The imperfection factor α, which is a function of the steel yield strength, and the non-dimensional slenderness $\bar{\lambda}_{LT,\theta,com}$ at high temperature are given by:

$$\alpha = 0.65\sqrt{\frac{235}{f_y}} \tag{4}$$

$$\bar{\lambda}_{LT,\theta,com} = \bar{\lambda}_{LT}\sqrt{\frac{k_{y,\theta,com}}{k_{E,\theta,com}}} \tag{5}$$

where $k_{E,\theta,com}$ is the reduction factor for the modulus of elasticity at the maximum steel temperature in the compression flange.

The non-dimensional slenderness $\bar{\lambda}_{LT}$ at room temperature is given by:

$$\bar{\lambda}_{LT} = \sqrt{\frac{W_{pl,y} f_y}{M_{cr}}} \tag{6}$$

where M_{cr} is the critical elastic moment at room temperature which causes stability failure due to lateral-torsional buckling.

Eurocode 3 does not provide any guidance on how to calculate M_{cr} and this is left entirely at the designer's discretion. The calculation of this value should take into consideration all the parameters such as the loading type and position, end boundary conditions and effect of lateral restraints to represent the actual structure being investigated. Section 2.2 addresses this situation for steel-timber hybrid structures with continuous elastic lateral restraints.

2.2. Critical elastic moment of beams with continuous lateral restraints

According to Timoshenko and Gere [10], the critical elastic buckling moment M_{cr} of a simply supported beam with doubly-symmetric cross-section under pure bending can be determined using the classical Equation (7). In this case, it is assumed that the ends of the beam are prevented from lateral translation and twist, but are free to warp and rotate laterally. Similarly, the critical elastic buckling moment M_{cr} of a beam with continuous elastic restraints can be determined using Equation (8) under the same loading and end boundary conditions, the derivation of which can be found in Trahair [11].

$$M_{cr} = \frac{n^2\pi^2 EI_z}{L^2}\sqrt{\frac{I_w}{I_z} + \frac{L^2 GI_t}{n^2\pi^2 EI_z}} \quad or \quad \sqrt{\frac{n^2\pi^2 EI_z}{L^2}\left(GI_t + \frac{n^2\pi^2 EI_w}{L^2}\right)} \tag{7}$$

$$\left[M_{cr} + \frac{kaL^2}{n^2\pi^2}\right]^2 = \left[\frac{n^2\pi^2 EI_z}{L^2} + \frac{kL^2}{n^2\pi^2}\right]\left[GI_t + \frac{n^2\pi^2 EI_w}{L^2} + \frac{ka^2L^2}{n^2\pi^2}\right] \tag{8}$$

In the above equations, I_z is the moment of inertia about the minor z-z axis, L is the laterally unbraced length, E is the elastic modulus of steel, G is the shear modulus of steel, I_w is the warping constant of the section, I_t is the torsional constant of the section, n is the mode of buckling, k is the uniform continuous elastic restraint stiffness, and a is the position of the restraint measured from the centroid of the section (restraints located above the centroidal axis towards compression flange are negative and those below are positive [11]). It is important to note that

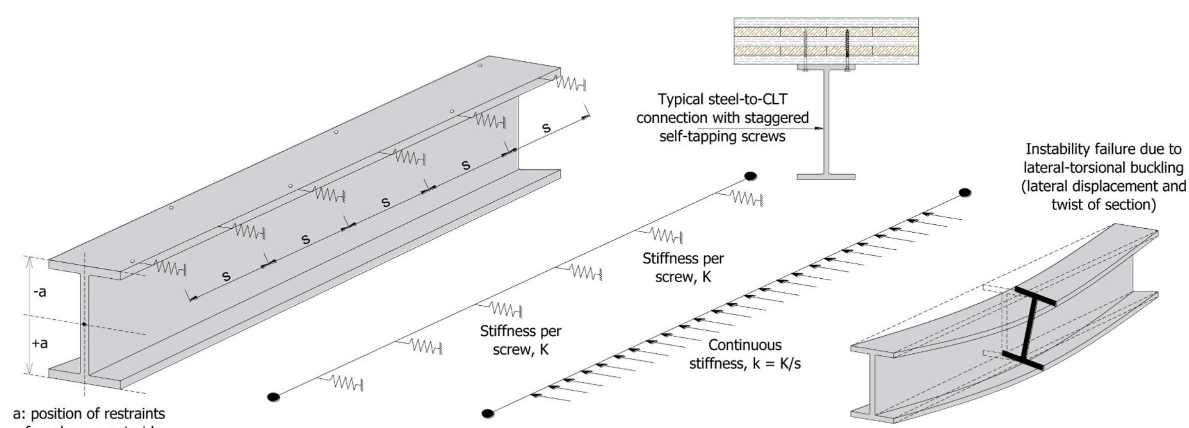

Fig. 1. Beam supported laterally by a continuous elastic medium.

the critical buckling mode of a continuously restrained beam is dependent on the degree of lateral restraint stiffness in contrast to an unrestrained beam for which the first mode gives the most critical situation for lateral-torsional buckling. Hence, several trials are required to determine the buckling mode which gives the lowest buckling moment for continuously restrained beams.

2.3. Lateral-torsional buckling resistance of beam-columns in fire

Steel beams, which are axially restrained at their ends as a result of the support conditions or the presence of adjacent members in a structure, develop axial compression due to restriction of the thermal expansion during the heating phase of a fire [3]. Members with a Class 1 or 2 cross-section that are subjected to combined uniaxial bending about the major axis $M_{y,fi,Ed}$ and axial compression $N_{fi,Ed}$ behave as beam-columns and should satisfy the following interaction equation:

$$\frac{N_{fi.Ed}}{\chi_{z,fi}Ak_{y,\theta}\frac{f_y}{\gamma_{M,fi}}}+\frac{k_{LT}M_{y,fi,Ed}}{\chi_{LT,fi}W_{pl,y}k_{y,\theta}\frac{f_y}{\gamma_{M,fi}}}\leq 1 \tag{9}$$

where $\chi_{z,fi}$ is a reduction factor for flexural buckling in fire situation, A is the area of the cross-section, and k_{LT} is an interaction factor for lateral-torsional buckling. $W_{el,y}$ should be used for Class 3 sections (see section 2.1 for other repeated notations).

The value of $\chi_{z,fi}$ is determined using the following equation:

$$\chi_{z,fi}=\frac{1}{\varphi_\theta+\sqrt{\varphi_\theta-\bar{\lambda}_\theta^2}} \tag{10}$$

with

$$\varphi_\theta=0.5\left[1+\alpha\bar{\lambda}_\theta+(\bar{\lambda}_\theta)^2\right] \tag{11}$$

The imperfection factor α is similar to that in Equation (4) and the non-dimensional slenderness $\bar{\lambda}_\theta$ at high temperature is given by:

$$\bar{\lambda}_\theta=\bar{\lambda}\sqrt{\frac{k_{y,\theta}}{k_{E,\theta}}} \tag{12}$$

The non-dimensional slenderness $\bar{\lambda}$ at room temperature is given by:

$$\bar{\lambda}=\sqrt{\frac{Af_y}{N_{cr}}} \tag{13}$$

where N_{cr} is the critical elastic buckling load at room temperature which causes stability failure and can be determined as explained later in Section 2.4.

The value of k_{LT} is found using the following equation:

$$k_{LT}=1-\frac{\mu_{LT}N_{fi,Ed}}{\chi_{z,fi}Ak_{y,\theta}\frac{f_y}{\gamma_{M,fi}}}\leq 1 \tag{14}$$

with

$$\mu_{LT}=0.15\bar{\lambda}_{z,\theta}\beta_{M,LT}-0.15\leq 0.9 \tag{15}$$

The value of $\beta_{M,LT}$ is equal to 1.1 for beams with pure bending with equal and opposite end moments, and 1.3 for beams with a uniformly distributed load.

2.4. Critical elastic load of columns with continuous lateral restraints

For a doubly-symmetric column with shear centre continuous elastic restraints k, the critical elastic load to cause lateral-torsional buckling can be determined using Equations (16)–(18), the derivation of which can be found in Trahair [11]. In this case, there are three possible buckling modes: flexure about the major y-y axis at $N_{cr,y}$, flexure about the minor z-z axis at $N_{cr,z}$, and torsion about the longitudinal x-x axis at $N_{cr,x}$. The actual buckling load N_{cr} will be the lowest of the three. In the equations, I_y is moment of inertia about the major y-y axis (see previous sections for other repeated notations).

$$N_{cr,y}=\frac{n^2EI_y}{L^2} \tag{16}$$

$$N_{cr,z}=\frac{n^2EI_z}{L^2}+\frac{kL^2}{n^2\pi^2} \tag{17}$$

$$N_{cr,x}=\frac{GI_t+\frac{n^2\pi^2EI_w}{L^2}}{r^2},\ with\quad r^2=\frac{I_y+I_z}{A} \tag{18}$$

For a doubly-symmetric column with continuous elastic restraints k acting at a distance a from the centroid of the section, a number of trials must be made to find the lowest buckling load N_{cr} using the general but more complex Equation (19). In many cases, the lowest solution will correspond to the flexural-torsional buckling mode in which the section twists and translates about the two axes [11].

$$N_{cr}=\min\left[\frac{n^2\pi^2EI_y}{L^2};\ \frac{(Ar^2+B)\pm\sqrt{(Ar^2+B)^2-4r^2(AB-C^2)}}{2r^2}\right] \tag{19}$$

with

$$A=\frac{kL^2}{n^2\pi^2}+\frac{n^2\pi^2EI_z}{L^2}\ ;\ B=\frac{ka^2L^2}{n^2\pi^2}+GI_t+\frac{n^2\pi^2EI_w}{L^2}\ ;\ C=-\frac{kaL^2}{n^2\pi^2} \tag{20}$$

3. Lateral restraint of steel-to-CLT connections

In current steel-timber hybrid construction, CLT floor panels are fixed to steel beams using regularly spaced self-tapping screws at spacings not exceeding 600 mm and in a staggered manner to prevent the potential for wood splitting during installation of the mechanical fasteners. The proprietary screws adopted in mass-timber connections are either partially threaded or fully threaded [1]. These screws offer a certain degree of lateral stiffness which can potentially prevent beam lateral-torsional buckling in both ambient and fire conditions. For conservatism in design, the steel beams can be designed as laterally unrestrained due to the uncertainty among designers on the current practice regarding the degree of lateral restraint offered by the screws, particularly under fire exposure. Merryday et al. [12] conducted a four-point bending test on a simply supported steel-CLT composite beam and reported that lateral-torsional buckling is not a concern at ambient temperature even with a narrow CLT slab width.

Over the years, numerous experimental tests have been carried out for timber-to-timber connections and several semi-empirical equations have been developed to predict their mechanical behaviour as given in design standards such as BS EN 1995-1-1:2004+A2 [13]. Conversely, experimental programmes for steel-to-timber connections using self-tapping screws are less established, especially under elevated temperatures in which most of the studies investigated connections made with bolts and dowels [14,15]. Researchers such as Hassanieh et al. [16], Loss et al. [17], Hassanieh et al. [18], Yang et al. [19] and Ling et al. [20] present several ambient temperature tests on various types of steel-to-timber connections, but these are generally not representative of the typical connection system adopted in current large-scale steel-timber hybrid construction. More realistic monotonic push-out tests using self-tapping screws to connect steel-CLT specimens have been carried out by MTC Solutions [21] and Merryday et al. [22], but these mainly focused on the connection strength rather than the lateral stiffness characteristics. On the other hand, Létourneau-Gagnon et al. [14] investigated the pull-out resistance of self-tapping screws via high temperature pull-out tests and also reported that limited information is available on the fire performance of such modern mass timber fasteners.

The load-slip relationship of steel-to-CLT connections using self-tapping screws is highly complex and is generally characterised by a non-linear behaviour at ambient temperature as shown in Fig. 2. For design purposes, the lateral stiffness offered by screws is defined in terms of the slip modulus for different limit states: K_{ser} for the serviceability limit state, K_u for the ultimate limit state and K_{fi} for the fire limit state. In accordance with BS EN 26891 [23], the slip modulus K_{ser} can be determined experimentally using Equation A as given in Table 1. Other semi-empirical expressions for stiffness can also be used to predict K_{ser} using Equations B, C, D1 and D2 in Table 1, and more detailed information on these equations can be found in Jockwer and Jorissen [24] and Jockwer et al. [25]. The determination of the slip modulus K_u is not specified in BS EN 26891 [23] and is taken as two-thirds of K_{ser} as per BS EN 1995-1-1:2004+A2 [13]. The slip modulus K_{fi} under fire condition should be taken as 20 % of K_u in line with BS EN 1995-1-2 [26]. This indicates that in fire, a single value of K_{fi} is applicable and no consideration is given to the connector degradation at different temperatures, as illustrated in Fig. 3. The degradation curve shown is only for the purpose of illustration (based on the general shape of shear connector strength reduction in steel-concrete composite structures) as there is a lack of experimental studies on the behaviour of such type of connection system in fire. High-temperature push-out tests are required to characterise the curve-shape, which will be influenced by the material degradation/failure criterion of the individual components of the connection. However, this connection design assumption can be problematic if it is a non-conservative simplification in terms of structural behaviour and should therefore be explicitly verified by fire testing, as the joint behaviour influences the force distribution and deformation of a structure.

For this study, the load-slip curves from the two aforementioned papers [21,22] were used to determine the slip modulus K_{ser}, as shown in Fig. 4. The results show that K_{ser} varies approximately between 1.50 kN/mm and 3.50 kN/mm per screw for the 12 mm nominal diameter self-tapping screws. From Fig. 5, it can also be observed that the experimental results obtained using Equation A generally deviate significantly from the predictions of Equations B, C, D1 and D2, with the exception of Equation C, which is reliable in some circumstances. Jockwer and Jorissen [24] also concluded that the background of the equations for stiffness in Eurocode 5 is vague and based on simplified assumptions. Hence, further research is required to develop clear guidelines on the mechanical performance of steel-to-timber connections using self-tapping screws, particularly in fire conditions. The fire testing should consider parameters such as the type of screw (partially or fully threaded), screw diameter, screw embedment length, screw spacing, outer grain orientation, panel layup and lamella thickness. This would enable designers to predict the lateral stiffness K_{fi} at various temperatures, which could subsequently be used to check the lateral-torsional buckling resistance of heated beams. At this stage of the present study, it is proposed to use Equation (21) to estimate the

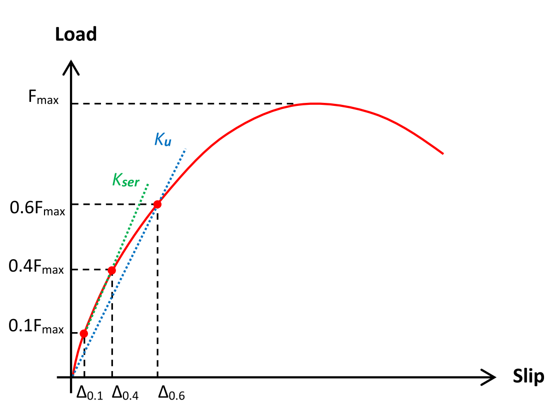

Fig. 2. Typical load-slip curve for steel-timber connection with self-tapping screws.

Table 1
Equations to calculate K_{ser}, K_u, and K_{fi} in N/mm.

	Equations	Reference
A	$K_{ser} = \dfrac{0.4F_{max}}{\frac{4}{3}(\nu_{04} - \nu_{01})}$	BS EN 26891 [23]
B	$K_{ser} = \dfrac{\rho_m{}^{1.5}d}{23}$ (*may be multiplied by* 2.0)	BS EN 1995-1-1:2004+A2 [13]
C	$K_{ser} = \dfrac{\rho_k{}^{1.5}d}{30}$	Ehlbeck and Larsen [27]
D1	$K_{ser,0} = 6\rho_k{}^{0.5}d^{1.7}$	SIA 265 [28]
D2	$K_{ser,90} = 3\rho_k{}^{0.5}d^{1.7}$	
E	$K_u = \frac{2}{3}K_{ser}$	BS EN 1995-1-1:2004+A2 [13]
F	$K_{fi} = 0.2K_u$	BS EN 1995-1-2 [26]

Where F_{max} is the maximum load.
ν_{04} and ν_{01} are the slip at 40 % and 10 % of the maximum load, respectively.
ρ_m is the mean density in kg/m^3.
ρ_k is the characteristic density in kg/m^3.
d is the nominal diameter of the screw in mm.

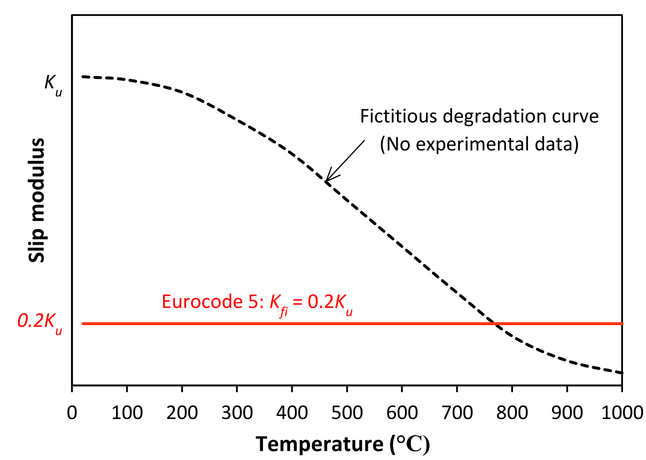

Fig. 3. Fictitious degradation curve of screws in fire and Eurocode 5 guidance.

serviceability slip modulus in the absence of more rigorous tests from screw manufacturers, from which K_{fi} could then be estimated. Equation (21) is based on Equation C in Table 1 but with the application of a correction factor of 0.5 to ensure conservatism in the absence of more definitive experimental or numerical data.

$$K_{ser} = \frac{\rho_k{}^{1.5}d}{60} \tag{21}$$

Table 2 shows the variation of the continuous lateral stiffness k_{fi} for the fire limit state with spacing of staggered self-tapping screws varying from 200 mm to 500 mm. These values have been determined for the range of slip modulus K_{ser} (1.50 kN/mm to 3.50 kN/mm) observed in the push-out tests. From the tabulated data, it can be inferred that k_{fi} has lower- and upper-bounds of approximately 500 kN/m/m and 2000 kN/m/m, respectively. These values represent the practical range of continuous lateral stiffness likely to be mobilised in steel-timber hybrid structures based on current design guidance and test datasets, which must evidently be validated with further fire experimentation.

4. Parametric study for downstand steel-timber hybrid systems

This section presents a parametric study performed on four steel beams and beam-columns in a downstand arrangement to investigate analytically the potential for lateral-torsional buckling under high temperatures. In line with current practice, it is assumed that the steel

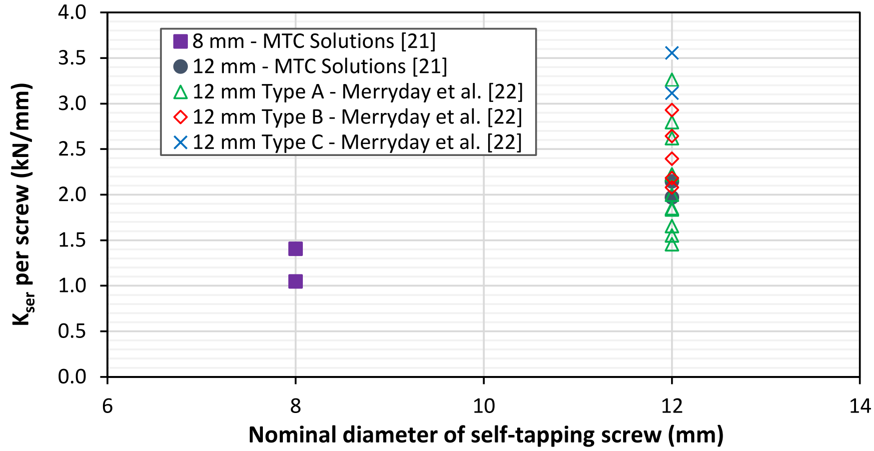

Fig. 4. Variation of K_{ser} with nominal diameter of self-tapping screws.

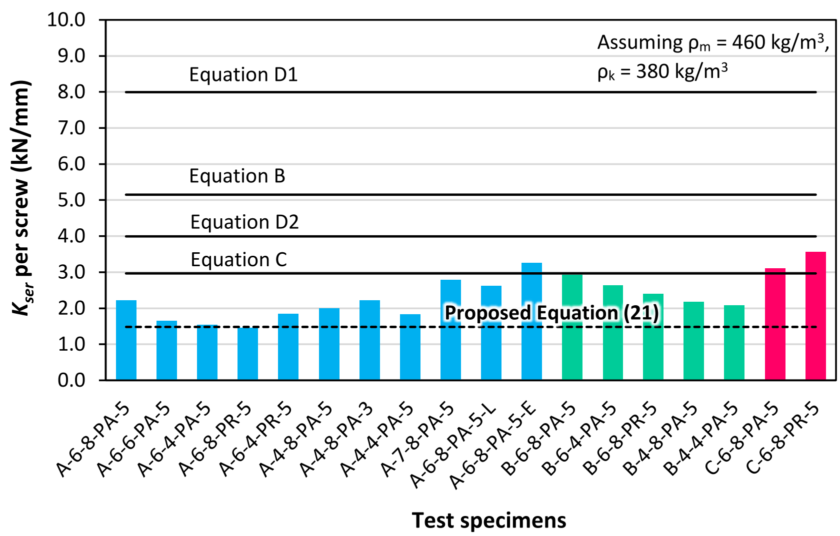

Fig. 5. Experimental and predicted K_{ser} for different test specimens in Merryday et al. [22].

Table 2
Continuous lateral stiffness k_{fi} in fire for different screw spacings.

K_{ser} (kN/mm)	1.50	2.00	2.50	3.00	3.50
K_u (kN/mm)	1.00	1.33	1.67	2.00	2.33
K_{fi}(kN/mm)	0.200	0.267	0.333	0.400	0.467
Spacing (mm)	**Continuous lateral stiffness, k_{fi} (kN/m/m)**				
200	1000	1333	1667	2000	2333
250	800	1067	1333	1600	1867
300	667	889	1111	1333	1556
350	571	762	952	1143	1333
400	500	667	833	1000	1167
450	444	593	741	889	1037
500	400	533	667	800	933

Note: The continuous lateral stiffness k_u at ambient temperature can be obtained by multiplying the tabulated values of k_{fi} by 5.

members carry all the applied loading and any form of composite action offered by the CLT slab is neglected because the degree of composite action mobilised in fire is not yet clearly understood. Hot-rolled structural steel members with a simply supported span of 9 m, steel grade S355, and span-to-depth ratios (L/H) of approximately 10, 15, 20 and 25 were selected for the present study. The 9 m span was chosen to reflect typical steel framing schematics with 9 m × 9 m column grids. Some of the key sectional and material properties of the steel cross-sections adopted are summarised in Table 3. Section classification was carried out for pure bending and for combined bending with axial compression for the fire limit state.

LTBeamN [29], which is a free finite element software and developed by CTICM, was used for the determination of the critical moment M_{cr} and critical load N_{cr} for various loading and continuous lateral restraint conditions. The software facilitates the calculation of the critical moment and load in complex situations not covered by standard expressions and the equations presented in Section 2.2 and 2.4 were verified by the output results under specific conditions. In all cases, it is assumed that the end boundary conditions of the steel members are prevented from lateral translation and twist, but are free to warp and

Table 3
Sectional and material properties of S355 steel members with 9 m span.

Steel member	L/H	$W_{pl,y}$ (cm^3)	$W_{el,y}$ (cm^3)	f_y (MPa)
UB 914 × 305 × 253	9.80	10944	9503	355
UB 610 × 229 × 125	14.71	3673	3219	355
UB 457 × 152 × 74	19.51	1624	1408	355
UB 356 × 171 × 57	25.10	1009	896	355

rotate laterally. These values were then used as input to determine the lateral-torsional buckling resistance of the steel beams and beam-columns in the fire situation. The parametric study was performed using a range of constant continuous lateral stiffness k (Fig. 1) from 100 kN/m/m to 50000 kN/m/m, representing the continuous lateral stiffness k_{fi} at the fire limit state as shown in Fig. 3. In reality, K_{fi} (and therefore k_{fi}) will vary with the screw temperature and more representative non-linear load-slip response of the screws must be considered for different temperatures to capture the mechanical response. However, it is presumed that the lateral torsional buckling resistance of beams and beam-columns obtained using this constant value ($K_{fi} = 0.2K_u$) from Eurocode 5 guidance is conservative, until more high temperature

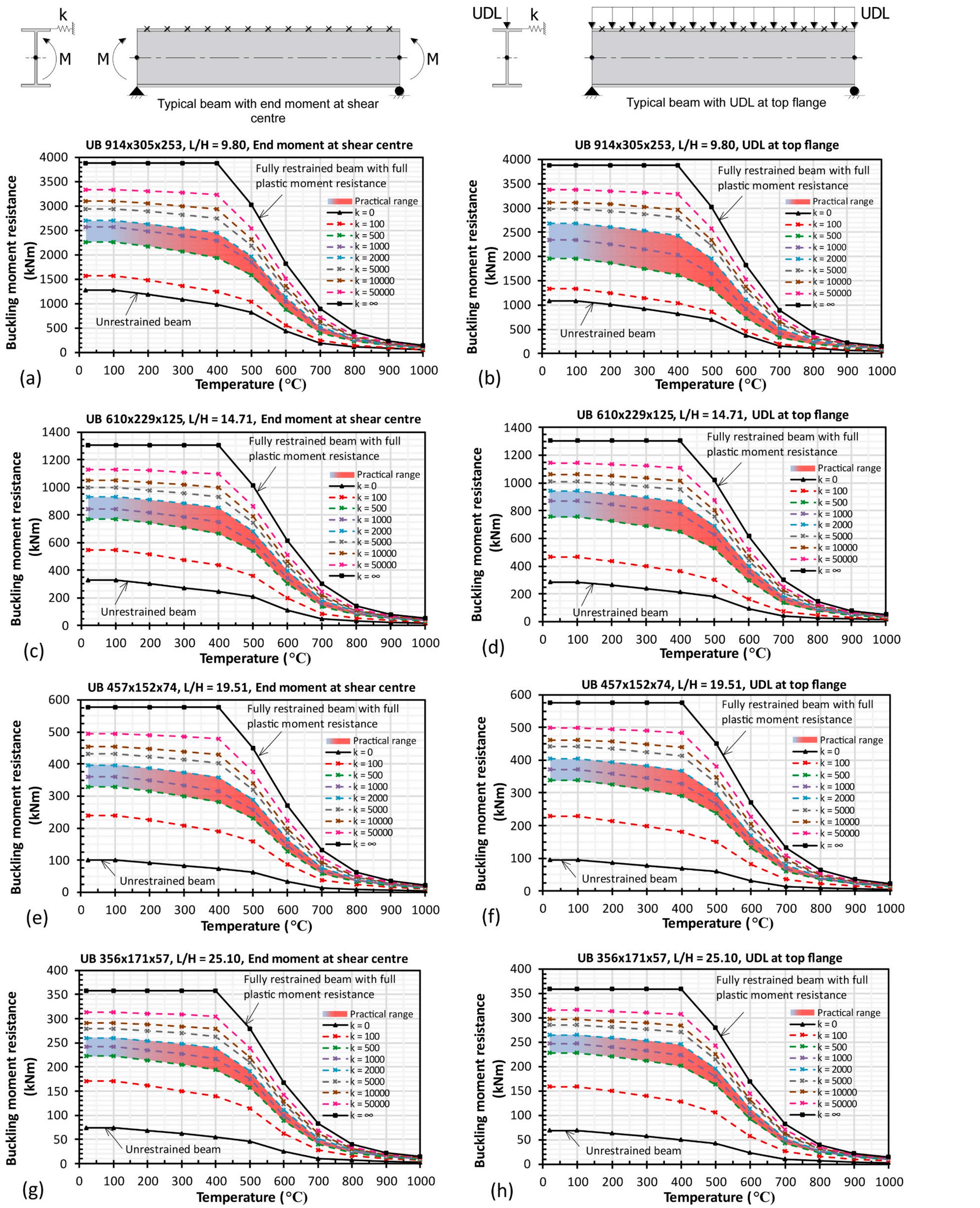

Fig. 6. Variation of buckling moment resistance of beams with temperature for different degree of restraints with moment for span-to-depth ratios (a) 9.80, (c) 14.71, (e) 19.51, and (g) 25.10 and uniformly distributed load for span-to-depth ratios (b) 9.80, (d) 14.71, (f) 19.51, and (h) 25.10.

research data are available to characterise such connection behaviour.

It must also be pointed out that the calculation methods presented in Section 2 can be applied under both uniform and non-uniform temperature distribution in the steel cross-section; BS EN 1993-1-2 [8] notes that it can conservatively be assumed that the compression flange temperature is equal to the uniform temperature. Hence, it is assumed that the reference temperature in this study is the temperature of the steel web as numerical simulations by Godoy Dellepiani et al. [30] have shown initial non-uniform temperature profile with a cooler compression flange in steel-timber hybrid structures until a relatively uniform temperature profile is achieved with increasing fire exposure time. This assumption is expected to lead to safe results at this stage of the study and future numerical investigations are required to assess the effect of non-uniform heating over the member cross-section on the response of such systems.

4.1. Beams

Two different loading conditions were considered for the four selected simply supported steel beams with free axial expansion under high temperatures: one with uniform end moment located at the shear centre and the other with a uniformly distributed load on the top flange. In both circumstances, it is assumed that the continuous elastic restraints representing the screws act at the top flange of the section. All the sections were found to be of Class 1 under pure bending in fire.

Fig. 6 illustrates the variation of the buckling moment resistance of the steel beams with increasing temperatures for different span-to-depth ratios. The upper- and lower-bound curves respectively represent a fully restrained beam with full plastic moment resistance and a laterally unrestrained beam with zero restraint. The shaded area between the two bounds with continuous lateral stiffness k of approximately 500 kN/m/m and 2000 kN/m/m represents the practical range of buckling moment resistance likely to be mobilised in steel-timber hybrid structures. Fig. 7 provides a more accurate distinction in terms of the ratio of the buckling moment resistance of a uniformly loaded beam with continuous lateral restraints to that of an unrestrained beam (Fig. 7a) or a fully restrained beam (Fig. 7b) with different span-to-depth ratios and temperatures. It can be observed that the ratio varies between 1.80 and 5.99 for unrestrained beams and between 0.36 and 0.75 for restrained beams.

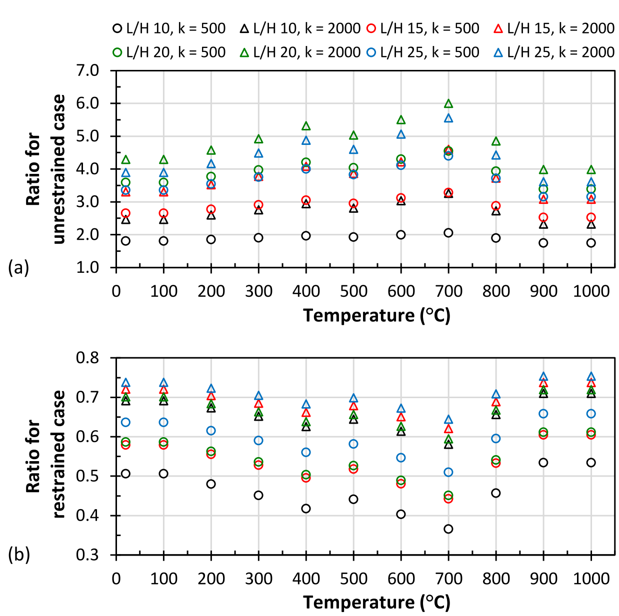

Fig. 7. Ratio of buckling moment resistance of beam with continuous lateral restraints to that of (a) unrestrained beam and (b) fully restrained beam under uniformly distributed load with temperature.

From the above findings and assuming fire is the governing limit state, it can be deduced that if steel beams are designed as unrestrained in fire conditions, they would have additional reserve strength at the fire limit state due to the presence of the continuous lateral restraints. As such, this may lead to material savings in steel and fire protection, subject to further investigations. However, if the beams are designed as fully restrained, they may fail by lateral-torsional buckling at a load much lower than the full plastic moment resistance assumed in the design. This means that relying entirely on the screws for full restraint conditions appears unrealistic and may result in unsafe structures in the event of a fire. Consequently, further experimental and/or numerical investigations are required to determine the applicability of the current design buckling resistance equations for steel members with continuous elastic restraints in fire. Such investigations are essential to establish the framework required for the design of steel-hybrid structures at elevated temperatures.

4.2. Beam-columns (beams with axial compression)

This section deals with axially restrained steel beams subject to uniaxial bending about the major axis $M_{y,fi,Ed}$ which develop axial compression $N_{fi,Ed}$ during heating. In this case, Equation (9) can be re-written as follows with axial and bending terms:

$$\frac{N_{fi,Ed}}{N_{b,fi,t,Rd}}+\frac{k_{LT}M_{y,fi,Ed}}{M_{b,fi,t,Rd}}\leq 1 \tag{22}$$

In Equation (22), $N_{b,fi,t,Rd}$ is the buckling resistance of a compression member, which is affected by the presence of continuous elastic restraints. This interaction formula reduces down to a beam problem when the axial compression is zero (as demonstrated previously in Section 4.1) and to a column with pure axial compression when there is no bending moment present. Hence, the influence of continuous elastic restraints on compression members must also be understood in order to account for combined bending and axial loading using Equation (22).

Fig. 8 illustrates the variation of the compression buckling resistance of four simply supported steel columns with increasing temperatures under the effect of axial compression acting at the shear centre and continuous elastic restraints located at the top flange of the section. It can be observed that such columns are particularly sensitive to the restraints, with continuous lateral stiffness k of approximately 500 kN/m/m approaching a fully restrained section at the top flange. An extreme value of k equal to 1×10^{18} kN/m/m was used as input in LTBeamN [29] to represent the situation with infinite lateral stiffness. As a result, such structural systems offer enhanced performance compared to unrestrained ones in terms of compression buckling resistance in fire conditions. It must be noted that the selected sections are Class 4 under pure compression and the equations described in Section 2.3 to determine $N_{b,fi,t,Rd}$ are not strictly applicable. On the contrary, these equations can still be used to verify buckling resistance for Class 1, 2 and 3 sections under combined bending and axial compression for a certain level of compression force.

To evaluate both bending moment and axial compression in combination, the effect of continuous elastic restraints acting at the top flange of the section on four simply supported beam-columns was investigated at temperatures of 500 °C, 600 °C and 700 °C. The sections were found to be of Class 1, 2 and 3 in fire, with the section classification depending on the level of applied axial compression as shown in Table 4.

Fig. 9 shows the interaction diagrams in terms of buckling moment resistance of the beam-columns with a uniformly distributed load on the top flange and axial compression acting at the shear centre of the section. The plotted curves define the failure envelope for all the possible combinations due to axial compression and bending for continuous lateral stiffness k of 0 kN/m/m, 500 kN/m/m and 2000 kN/m/m. The kink observed in Fig. 9a and b, with sudden drop in buckling moment resistance, indicates a change in section class from Class 2 to Class 3. As

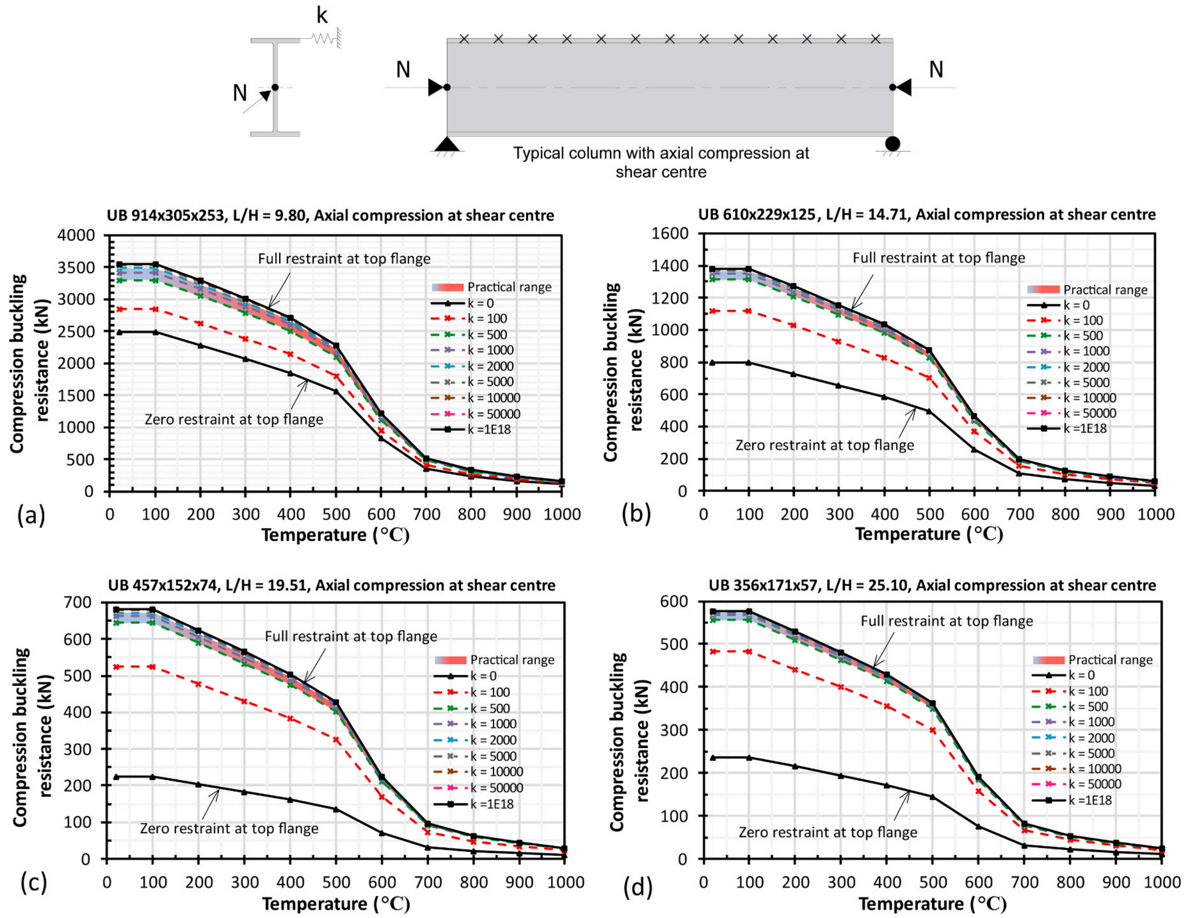

Fig. 8. Variation of compression buckling resistance with temperature for different degree of restraints and span-to-depth ratios of (a) 9.80, (b) 14.71, (c) 19.51, and (d) 25.10.

Table 4
Section classification based on maximum axial compression force.

Steel member	L/H	Maximum axial compression (kN)			
		Class 1	Class 2	Class 3	Applied
UB 914 × 305 × 253	9.80	192	871	4683	2234
UB 610 × 229 × 125	14.71	161	482	2490	862
UB 457 × 152 × 74	19.51	203	412	1749	420
UB 356 × 171 × 57	25.10	223	372	1621	360

mentioned previously, the sections become Class 4 under pure compression and the compression resistance on the interaction diagrams should be recalculated accordingly, which is outside the scope of this study. However, the purpose of this investigation is to illustrate the shift and improvement of moment-axial interaction diagrams for the practical range of 500 °C to 700 °C of steel beam-columns under the effect of continuous elastic restraints in comparison to an unrestrained case, with the value of *k* equal to zero. It can be observed that the beam-columns with continuous restraints offer enhanced structural fire performance.

5. Conclusions

The influence of uniform continuous elastic restraints on steel beams and beam-columns in steel-timber hybrid structures at high temperature has been investigated. Based on the results of this investigation, the following conclusions can be drawn:

- Eurocode 3 provides design equations to check the lateral-torsional buckling resistance of steel beams and beam-columns at high temperatures. However, further experimental and/or numerical investigations are required to determine the applicability of these equations for steel members with continuous elastic restraints in fire and to identify whether they are overly conservative or unsafe.
- Prediction equations for the slip modulus of self-tapping screws at ambient temperature generally deviate significantly from experimental results and the assumption of 80 % reduction of the slip modulus given in Eurocode 5 under fire conditions must be verified with further testing for steel-to-CLT connections using self-tapping screws, as also recommended in Ref. [2].
- If fire is the governing limit state, designing simply supported steel beams with free axial expansion as laterally restrained in fire conditions appears to be unrealistic and may lead to unsafe structures. On the other hand, designing beams as unrestrained indicates some reserve capacity, offering the possibility of material reduction in steel and fire protection.
- The presence of continuous lateral restraints in simply supported steel beam-columns shows an improvement of the moment-axial interaction diagrams at 500 °C, 600 °C and 700 °C compared to the unrestrained case.

This research has demonstrated that there is a significant lack of knowledge concerning steel-timber hybrid structures in fire. There is an urgent need for an experimental campaign of elevated temperature push-out tests to evaluate the longitudinal shear performance of modern screw connections in cross-laminated timber subjected to fire. With this data, a better understanding of steel-timber composite beams in fire can be developed using the tools outlined in this paper. To date, only numerical studies of steel-timber hybrid structures have been conducted in

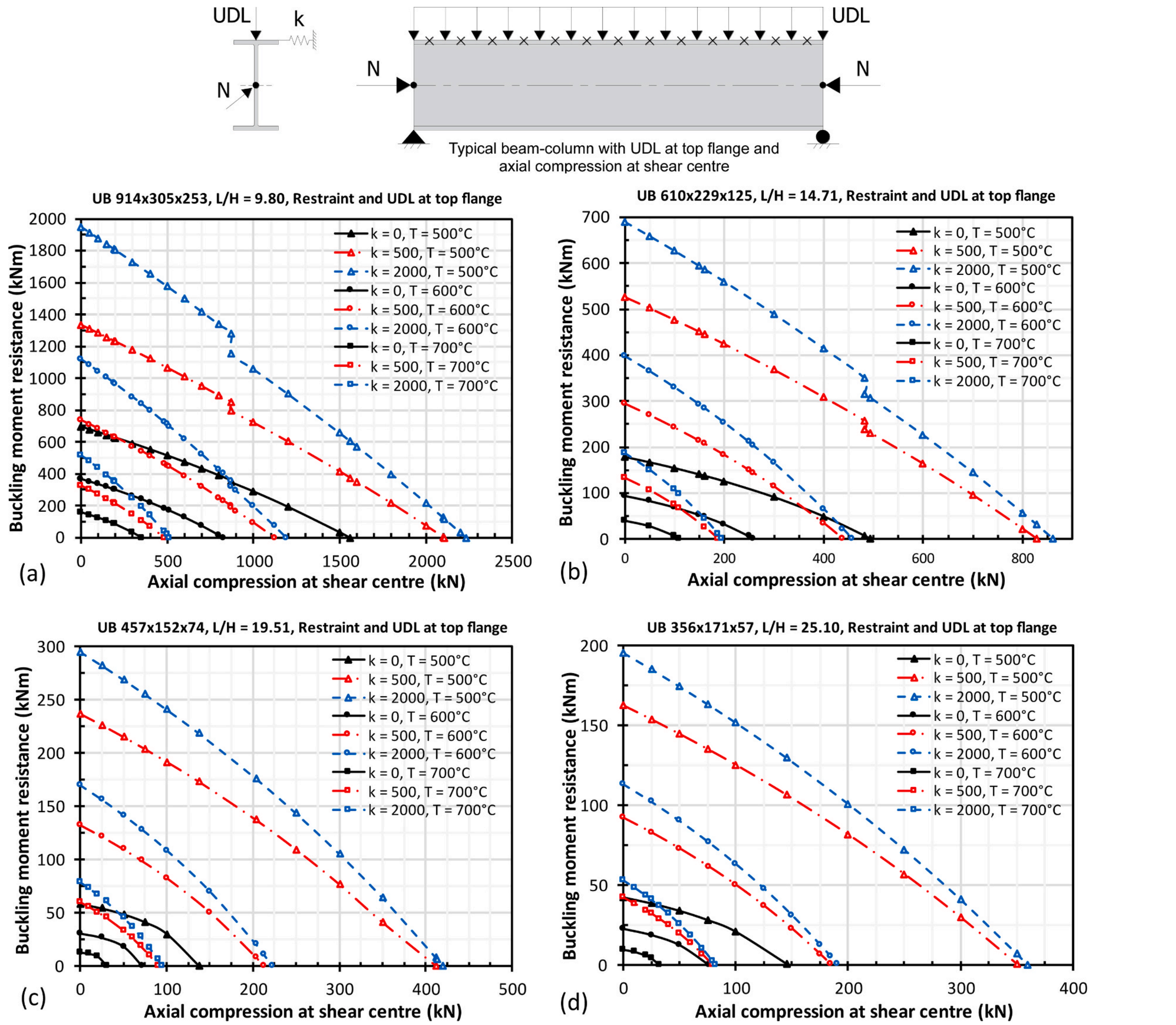

Fig. 9. Interaction diagrams at 500, 600 and 700 °C for continuous lateral stiffness k of 0, 500 and 2000 kN/m/m for span-to-depth ratios (a) 9.80, (b) 14.71, (c) 19.51, and (d) 25.10.

fire and there is a clear need for complementary experimental work as the demand for this hybrid topology is increasing in the built environment.

CRediT authorship contribution statement

Aatish Jeebodh: Writing – original draft, Visualization, Methodology, Formal analysis, Data curation, Conceptualization. **Buick Davison:** Writing – review & editing, Supervision, Project administration, Methodology, Funding acquisition, Conceptualization. **Martyn S. McLaggan:** Writing – review & editing, Supervision, Project administration, Methodology, Funding acquisition, Conceptualization. **Ian Burgess:** Writing – review & editing, Supervision, Project administration, Methodology, Funding acquisition, Conceptualization. **Danny Hopkin:** Writing – review & editing, Supervision, Project administration, Methodology, Funding acquisition, Conceptualization. **Shan-Shan Huang:** Writing – review & editing, Supervision, Project administration, Methodology, Funding acquisition, Conceptualization.

Declaration of competing interest

The authors declare that they have no known competing financial interests or personal relationships that could have appeared to influence the work reported in this paper.

Data availability

Data will be made available on request.

Acknowledgements

This work was supported by the UK Engineering and Physical Sciences Research Council [grant number EP/T517835/1] in collaboration with OFR Consultants.

References

[1] D. Barber, et al., Design Guide 37: Hybrid Steel Frames with Wood Floors, American Institute of Steel Construction, USA, 2022.

[2] D. Barber, A. Roy-Poirier, L. Wingo, Modelling the fire performance of steel beam to CLT connections for hybrid construction, in: Proceedings of the 12th Asia-Oceania Symposium on Fire Science and Technology (AOSFST 2021), Brisbane, Australia, 2021, https://doi.org/10.14264/E58A1CA.

[3] G.-Q. Li, S.-X. Guo, Experiment on restrained steel beams subjected to heating and cooling, J. Constr. Steel Res. 64 (3) (2008/03/01/2008) 268–274, https://doi.org/10.1016/j.jcsr.2007.07.007.

[4] A.R. Flint, *The Influence of Restraints on the Stability of Beams* (No. 29(9)), The Structural Engineer, 1951.
[5] F. McCann, L. Gardner, M.A. Wadee, Design of steel beams with discrete lateral restraints, J. Constr. Steel Res. 80 (2013/01/01/2013) 82–90, https://doi.org/10.1016/j.jcsr.2012.09.011.
[6] T. Belaid, F. Ammari, R. Adman, Influence of load position on critical lateral torsional buckling moment of laterally restrained beam at tense flange, Asian Journal of Civil Engineering 19 (7) (2018/11/01 2018) 839–848, https://doi.org/10.1007/s42107-018-0067-7.
[7] P.M.M. Vila Real, R. Cazeli, L. Simões da Silva, A. Santiago, P. Piloto, The effect of residual stresses in the lateral-torsional buckling of steel I-beams at elevated temperature, J. Constr. Steel Res. 60 (3) (2004) 783–793, https://doi.org/10.1016/S0143-974X(03)00143-3, 2004/03/01/.
[8] BS EN 1993-1-2, Eurocode 3: Design of Steel Structures - Part 1-2: General Rules - Structural Fire Design, British Standards Institution, 2005.
[9] J.-M. Franssen, P. Vila Real, in: Multicomp Lda, Mem Martins (Eds.), Fire Design of Steel Structures, second ed., ECCS and Ernst & Sohn, Portugal, 2015.
[10] S.P. Timoshenko, J.M. Gere, Theory of Elastic Stability, second ed. ed., McGraw-Hill Book Company, Inc., 1961.
[11] N.S. Trahair, Flexural-Torsional Buckling of Structures, CRC Press, Boca Raton, 1993.
[12] H. Merryday, M. Potuzak, D. Roueche, K. Sener, Experimental and numerical investigations on the usage of CLT panels to form timber-steel composite floor systems, in: World Conference on Timber Engineering (WCTE 2023), Oslo, Norway, 2023, pp. 3373–3381, https://doi.org/10.52202/069179-0439.
[13] BS EN 1995-1-1:2004+A2, Eurocode 5: Design of Timber Structures - Part 1-1: General - Common Rules and Rules for Buildings, British Standards Institution, 2014.
[14] M. Létourneau-Gagnon, C. Dagenais, P. Blanchet, Fire performance of self-tapping screws in Tall mass-timber buildings, Appl. Sci. 11 (8) (2021) 3579, https://doi.org/10.3390/app11083579.
[15] A.C. Marcolan Júnior, P. Dias de Moraes, Probabilistic model for determining the failure time of steel-to-timber connections with multiple dowel-type fasteners exposed to fire, Fire Saf. J. 133 (2022/10/01/2022) 103646, https://doi.org/10.1016/j.firesaf.2022.103646.
[16] A. Hassanieh, H.R. Valipour, M.A. Bradford, Load-slip behaviour of steel-cross laminated timber (CLT) composite connections, J. Constr. Steel Res. 122 (2016/07/01/2016) 110–121, https://doi.org/10.1016/j.jcsr.2016.03.008.
[17] C. Loss, M. Piazza, R. Zandonini, Connections for steel-timber hybrid prefabricated buildings. Part I: experimental tests, Construct. Build. Mater. 122 (2016) 781–795, https://doi.org/10.1016/j.conbuildmat.2015.12.002, 09/30.
[18] A. Hassanieh, H.R. Valipour, M.A. Bradford, Composite connections between CLT slab and steel beam: Experiments and empirical models, J. Constr. Steel Res. 138 (2017/11/01/2017) 823–836, https://doi.org/10.1016/j.jcsr.2017.09.002.
[19] R. Yang, H. Li, R. Lorenzo, M. Ashraf, Y.-f. Sun, Q. Yuan, Mechanical behaviour of steel timber composite shear connections, Construct. Build. Mater. (2020), https://doi.org/10.1016/j.conbuildmat.2020.119605.
[20] Z. Ling, X. Rong, Z. Xiang, Laterally loaded performance of single dowel-type fastener used for steel plate-to-timber connections, Structures 34 (2021/12/01/2021) 1985–1997, https://doi.org/10.1016/j.istruc.2021.08.115.
[21] MTC Solutions, Steel to CLT Lateral Connections, MyTiCon Timber Connectors, Surrey, BC, Canada, 2019 [Online]. Available: https://mtcsolutions.com/resources/white-papers/steel-to-clt-lateral-connections/.
[22] H.C. Merryday, K. Sener, D. Roueche, Pushout tests on steel-timber connections using self-tapping screws, Structures Congress 2023 (2023) 312–327, https://doi.org/10.1061/9780784484777.028.
[23] BS EN 26891, Timber Structures. Joints Made with Mechanical Fasteners. General Principles for the Determination of Strength and Deformation Characteristics, British Standards Institution, 1991.
[24] R. Jockwer, A. Jorissen, Stiffness and Deformation of Connections with Dowel-type Fasteners " in "Design of Connections in Timber Structures: A State-Of-The-Art Report by COST Action FP1402/WG3, Shaker Verlag, 2018.
[25] R. Jockwer, D. Caprio, A. Jorissen, Evaluation of parameters influencing the load-deformation behaviour of connections with laterally loaded dowel-type fasteners, Wood Mater. Sci. Eng. 17 (1) (2022/01/02 2022) 6–19, https://doi.org/10.1080/17480272.2021.1955297.
[26] BS EN 1995-1-2, Eurocode 5: Design of Timber Structures - Part 1-2: General - Structural Fire Design, British Standards Institution, 2004.
[27] J. Ehlbeck, H.J. Larsen, Eurocode 5 - design of timber structures: joints, in: Presented at the International Workshop on Wood Connectors., Madison, WI, United States, 1993 [Online]. Available: https://www.cost.eu/uploads/2018/11/Design-of-Connections-in-Timber-Structures.pdf.
[28] SIA 265, *Timber Structures*, SIA Swiss Society of Engineers and Architects, Zurich, Switzerland, 2012.
[29] CTICM, Logiciel LTBeamN – Déversement élastique de poutres fléchies comprimées, 2023 [Online], https://www.cticm.com/logiciel/ltbeamn/.
[30] M. Godoy Dellepiani, G. Roa Munoz, S.J. Yanez, C.F. Guzmán, E.I. Saavedra Flores, J.C. Pina, Numerical study of the thermo-mechanical behavior of steel–timber structures exposed to fire, J. Build. Eng. 65 (2023/04/15/2023) 105758, https://doi.org/10.1016/j.jobe.2022.105758.